



# Complement C1q mediates the expansion of periportal hepatic progenitor cells in senescence-associated inflammatory liver

Tung-Ching Ho<sup>a</sup>, Er-Yea Wang<sup>a</sup>, Kun-Huei Yeh<sup>b</sup>, Yung-Ming Jeng<sup>c</sup>, Jau-Hau Horng<sup>a</sup>, Li-Ling Wu<sup>d</sup>, Yi-Tzu Chen<sup>a</sup>, Hsuan-Cheng Huang<sup>e</sup>, Chia-Lang Hsu<sup>b</sup>, Pei-Jer Chen<sup>f,g,h</sup>, Shiou-Hwei Yeh<sup>a,f,i,1</sup>, and Ding-Shinn Chen<sup>g,h,j,1</sup>

<sup>a</sup>Department and Graduate Institute of Medical Microbiology, National Taiwan University, 100 Taipei, Taiwan; <sup>b</sup>Graduate Institute of Clinical Oncology, National Taiwan University, 100 Taipei, Taiwan; <sup>c</sup>Graduate Institute of Pathology, National Taiwan University, 100 Taipei, Taiwan; <sup>d</sup>Institute of Physiology, National Yang-Ming University, 112 Taipei, Taiwan; <sup>e</sup>Institute of Biomedical Informatics and Center for Systems and Synthetic Biology, National Yang-Ming University, 112 Taipei, Taiwan; <sup>f</sup>Center for Genomic Medicine, National Taiwan University, 100 Taipei, Taiwan; <sup>g</sup>Graduate Institute of Clinical Medicine, National Taiwan University Hospital and National Taiwan University College of Medicine, 100 Taipei, Taiwan; <sup>h</sup>Department of Internal Medicine, National Taiwan University Hospital and National Taiwan University College of Medicine, 100 Taipei, Taiwan; <sup>i</sup>Department of Laboratory Medicine, National Taiwan University Hospital and National Taiwan University College of Medicine, 100 Taipei, Taiwan; and <sup>j</sup>Genomics Research Center, Academia Sinica, 115 Taipei, Taiwan

Contributed by Ding-Shinn Chen, January 24, 2020 (sent for review October 15, 2019; reviewed by Gen-Sheng Feng and Hironori Koga)

**Most hepatocellular carcinomas (HCCs) develop in patients with chronic hepatitis, which creates a microenvironment for the growth of hepatic progenitor cells (HPCs) at the periportal area and subsequent development of HCCs. We investigated the signal from the inflammatory liver for this pathogenic process in the hepatic conditional  $\beta$ -catenin knockout mouse model. Senescent  $\beta$ -catenin-depleted hepatocytes in aged mice create an inflammatory microenvironment that stimulates periportal HPC expansion but arrests differentiation, which predisposes mice to the development of liver tumors. The release of complement C1q from macrophages in the inflammatory niche was identified as the unorthodox signal that activated the  $\beta$ -catenin pathway in periportal HPCs and was responsible for their expansion and de-differentiation. C1q inhibitors blocked the  $\beta$ -catenin pathway in both the expanding HPCs and the liver tumors but spared its orthodox pathway in pericentral normal hepatocytes. This mechanism has been validated in human liver specimens from patients with chronic hepatitis. Taken together, these results demonstrate that C1q-mediated activation of  $\beta$ -catenin pathway in periportal HPCs is a previously unrecognized mechanism for replenishing hepatocytes in the inflammatory liver and, if unchecked, for promoting hepatocarcinogenesis. C1q may become a new target for blocking carcinogenesis in patients with chronic hepatitis.**

inflammation | microenvironment | periportal | progenitor cell | liver cancer

**M**ost cases of hepatocellular carcinoma (HCC) emerge after decades of chronic hepatitis, induced by either viral infections or by noninfectious etiology, before the final presentation as cancer (1). Therefore, a common pathway for HCC development involves chronic hepatitis as the microenvironmental factor that predisposes to liver tumors (2). Understanding the mechanism of how chronic hepatitis induces the transformation of hepatocytes to cancer cells is essential to identify new therapeutic targets.

Because chronic hepatitis results in hepatocyte death, regeneration is required to replace the damaged cells and maintain liver function. Repeated cycles of hepatitis and regeneration select cells with a growth advantage to form expanding clones and eventually form HCCs. Therefore, the origins of these regenerating cells in the liver and the signal from the inflammatory microenvironment to stimulate their regeneration are closely related to carcinogenesis and subject to investigation.

In normal liver cell turnover, newly generated hepatocytes have long been considered to derive from replication-competent mature hepatocytes (3). However, the regenerative activity of these cells decreases in the liver of patients with chronic hepatitis (4, 5); instead, the progenitor cells located around the portal

veins are found to be the main source for promoting compensatory liver regeneration. Based on the evidence from several recent studies, two different subgroups of periportal cells are responsible for liver regeneration, depending on the severity of liver diseases (6, 7). In subjects with mild liver damage, a subgroup of periportal Sox9<sup>+</sup> HNF4 $\alpha$ <sup>+</sup> hybrid hepatocytes replenish the injured liver but do not produce HCCs (7). In cases of severe liver injury, in which the majority of hepatocytes lose their regenerative potential and eventually undergo senescence, the hepatic progenitor cells (HPCs) at the canal of Hering are activated to repopulate the damaged liver, usually accompanied by ductular reactions. Expansion of this group of HPCs leads to liver tumor formation (8, 9).

In humans, many HCCs develop in the liver following a severe ductular reaction, in which ~50% of cirrhotic nodules and HCCs may be derived from the expanded HPCs that retain the expression of the progenitor cell markers CK19, OV6, and EpCAM (6). Thus, researchers have focused on replacement of the severely injured liver by periportal HPCs in patients with chronic hepatitis. The accumulation of senescent hepatocytes has been demonstrated in most advanced chronic liver diseases (10) and affects

## Significance

**This study has identified C1q in the chronic hepatitis liver as an unorthodox signal for activating the essential  $\beta$ -catenin pathway in hepatic progenitor cells (HPCs) and liver tumors, which is critical for their proliferation and dedifferentiation. Inhibition of C1q not only effectively suppressed the expansion, but also facilitated the differentiation of HPCs and liver tumors. However, it spared the orthodox  $\beta$ -catenin function in pericentral normal hepatocytes. C1q thus becomes a potential therapeutic target for liver tumors derived from HPCs in patients with chronic hepatitis.**

Author contributions: T.-C.H., E.-Y.W., K.-H.Y., P.-J.C., S.-H.Y., and D.-S.C. designed research; T.-C.H., E.-Y.W., J.-H.H., L.-L.W., and Y.-T.C. performed research; T.-C.H., E.-Y.W., K.-H.Y., Y.-M.J., H.-C.H., C.-L.H., P.-J.C., and S.-H.Y. analyzed data; and T.-C.H., E.-Y.W., P.-J.C., S.-H.Y., and D.-S.C. wrote the paper.

Reviewers: G.-S.F., University of California San Diego; and H.K., Kurume University School of Medicine.

The authors declare no competing interest.

Published under the [PNAS license](#).

<sup>1</sup>To whom correspondence may be addressed. Email: shyeh@ntu.edu.tw or chends@ntu.edu.tw.

This article contains supporting information online at <https://www.pnas.org/lookup/suppl/doi:10.1073/pnas.1918028117/-DCSupplemental>.

First published March 5, 2020.

disease progression through a substantial influence on the inflammatory microenvironment (11). Whether the senescent hepatocyte-induced inflammation affects the expansion and carcinogenesis of periportal HPCs and the underlying mechanism merits extensive study.

In the present study, we used the conditional  $\beta$ -catenin knockout mouse model to investigate the mechanism by which senescence-related chronic hepatitis induces the proliferation and carcinogenesis of periportal HPCs. In this model, neither the pericentral self-renewable cells nor the mature hepatocytes regenerate, because of depletion of the essential  $\beta$ -catenin. As shown in our previous study, a compensatory regeneration of HPCs occurs from 8 to 9 mo, which is approximately the end of the hepatocytes' life span. The liver parenchyma is replaced by the expanding HPCs in association with severe ductular reactions; the growing HPCs remain undifferentiated and develop liver tumors (12). Using this animal model, Russell et al. (13) consistently demonstrated that  $\beta$ -catenin is also important for liver regeneration after a choline-deficient, ethionine-supplemented diet-induced liver injury, and biliary epithelial cell-derived hepatocytes repopulate the liver during recovery. In the present study, we found that the senescence-associated inflammatory microenvironment predisposes the liver to the expansion of HPCs from periportal area. Thus, this mouse model appropriately recapitulates the expansion and carcinogenesis of periportal HPCs from the severe senescence type of human liver diseases. Using this animal model, we identified C1q as the key factor from the inflammatory liver that unorthodoxly activates the  $\beta$ -catenin pathway and is critical for the expansion and differentiation of periportal HPCs. Inhibition of C1q effectively reverses the HPC phenotypes in this mouse model.

## Results

**Aging  $\beta$ -Catenin-Depleted Hepatocytes Undergo Senescence and Induce an Inflammatory Microenvironment for HPC Expansion in the Mouse Liver.** To examine whether senescence-induced inflammation predisposed the liver to the expansion of HPCs in  $\beta$ -catenin KO mice, liver sections obtained from the mice at different ages were processed to check the senescence and inflammation status. By staining with antibodies against senescence markers, including  $\beta$ -galactosidase (SA- $\beta$ -gal), p21, and p16, we first noted that some senescent hepatocytes started to appear in the livers of 6- to 7-mo-old male  $\beta$ -catenin KO mice and were surrounded by inflammatory cells (Fig. 1A and B). The number of senescent hepatocytes gradually increased thereafter and peaked at 8 to 12 mo, as indicated by immunohistochemistry (IHC) staining for senescence markers (Fig. 1C and *SI Appendix*, Fig. S1) and the elevated p21 expression levels (Fig. 1D for mRNA; Fig. 1E for protein).

Meanwhile, the expression of the senescence-associated secretory phenotype (SASP) factor CCL2, which plays a key role in recruiting inflammatory cells (14), was also elevated along with the increase in senescent cells (Fig. 1F). An enrichment of inflammatory cells in the livers of  $\beta$ -catenin KO mice age >8 mo was demonstrated by hematoxylin and eosin (H&E) and CD45 staining (*SI Appendix*, Fig. S2A and B). Flow cytometry analysis further indicated increases in the numbers of infiltrating monocytes and lymphocytes in the 10-mo-old  $\beta$ -catenin KO mouse livers (Fig. 1G), with the increased CD11b<sup>+</sup> monocytes mainly the Ly6C<sup>+</sup> subsets of proinflammatory monocytes (*SI Appendix*, Fig. S3). This pattern is consistent with the documented pattern induced by senescent hepatocytes in the liver (15, 16). These results thus support the existence of an inflammatory microenvironment in this animal model at the end of the hepatocyte life span (~8 to 9 mo) that is associated with the senescence of  $\beta$ -catenin (-) hepatocytes.

As shown in our previous study, HPCs in the  $\beta$ -catenin KO liver remain  $\beta$ -catenin-positive, in contrast to hepatocytes that lose  $\beta$ -catenin expression by 2 wk after birth (12). This difference is due to the low albumin promoter activity in the undifferentiated

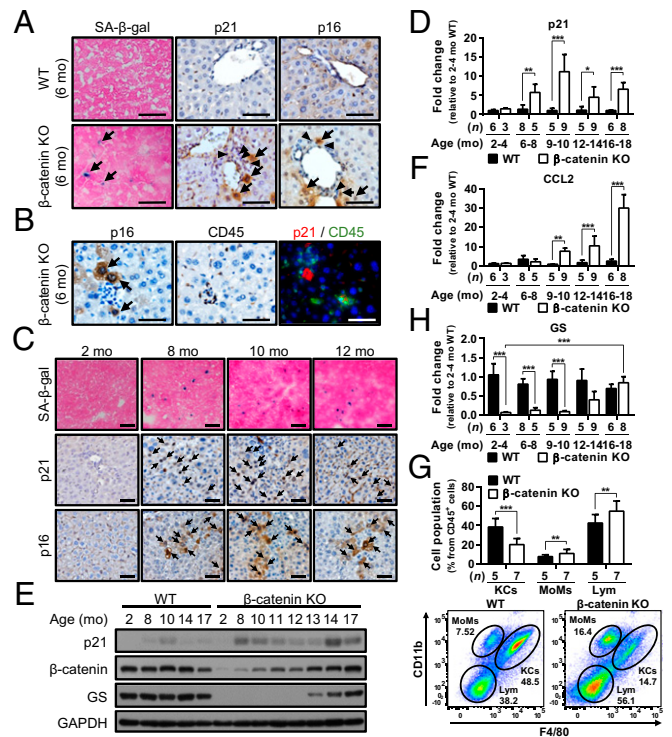


**Fig. 1.** Aging  $\beta$ -catenin-depleted hepatocytes undergo senescence and induce inflammatory cell infiltration for HPC expansion in  $\beta$ -catenin KO mice. (A–C) Representative images of IHC and IF staining for SA- $\beta$ -gal, p21, p16, and CD45 in the liver tissues of 6-mo-old WT mice, 6-mo-old  $\beta$ -catenin KO mice (A and B), and 2- to 12-mo-old  $\beta$ -catenin KO mice (C). The two IHC stainings for p16 and CD45 shown in B are in consecutive sections. Black arrows indicate positive signals; black arrowheads indicate inflammatory cells. (D) qRT-PCR data showing p21 expression in WT and  $\beta$ -catenin KO mice at the indicated ages. (E) Representative Western blots showing p21,  $\beta$ -catenin, and GS expression in WT (control) and  $\beta$ -catenin KO mice at the indicated ages. (F) qRT-PCR data showing CCL2 expression in WT and  $\beta$ -catenin KO mice at the indicated ages. (G) Immunophenotyping and quantification of liver-infiltrating immune cells by flow cytometry analysis of 10-mo-old WT and  $\beta$ -catenin KO mice, with the quantification results. KCs, Kupffer cells; MoMs, monocytes; Lym, lymphocytes. (H) qRT-PCR data showing GS expression in WT and  $\beta$ -catenin KO mice at the indicated ages. Results are shown as mean  $\pm$  SD. \* $P$  < 0.05; \*\* $P$  < 0.01; \*\*\* $P$  < 0.001. (Scale bars: 50  $\mu$ m.)

HPCs, resulting in lower expression of Cre that is insufficient for Cre-mediated depletion of the  $\beta$ -catenin gene. Therefore, the undifferentiated HPCs proliferating in the  $\beta$ -catenin KO liver remain  $\beta$ -catenin (+). Elevated expression levels of  $\beta$ -catenin and also of its downstream target gene, glutamine synthetase (GS), following the increases in p21 and CCL2 were found in  $\beta$ -catenin KO livers (Fig. 1E for protein; Fig. 1H for mRNA). In fact, the concurrent presence of the senescent  $\beta$ -catenin (-) mature hepatocytes and proliferating  $\beta$ -catenin (+) HPCs were well demonstrated by immunofluorescence (IF) staining for  $\beta$ -catenin with either Ki67 or p21 in the livers of  $\beta$ -catenin KO mice (*SI Appendix*, Fig. S4). Taken together, these results supported the establishment of a senescence-induced inflammatory niche in the  $\beta$ -catenin KO mice, which predisposed the liver for subsequent expansion of HPCs.

**Expansion of HPCs Associates with Bile Ductular Reactions at the Periportal Area in the Inflammatory Microenvironment.** As mentioned above, the expression of  $\beta$ -catenin becomes an indicator of undifferentiated HPCs proliferating in the  $\beta$ -catenin KO liver. Therefore, with the aim of identifying any zonal pattern of the



HPCs expanding in the inflammatory liver, the growth pattern of  $\beta$ -catenin (+) HPCs was inspected in the liver tissues from  $\beta$ -catenin KO mice at different ages by IF staining with the  $\beta$ -catenin antibody.

The  $\beta$ -catenin (+) HPCs started to appear in 6- to 7-mo-old mice around the periportal area (marked as CK19<sup>+</sup> bile ducts) and gradually expanded toward the central vein until they replaced almost the whole liver in 16- to 18-mo-old mice (Fig. 2A). The expansion of  $\beta$ -catenin (+) HPCs was associated with severe ductular reactions (Fig. 2A; increasing numbers of CK19-positive cholangiocytes), suggesting the origin cells of the expanding HPCs as bipotential ones for differentiation into either hepatocytes or cholangiocytes.

The oval cells at portal area are well documented as origin progenitor cells with the capability of bilineage differentiation, which expand in the liver with chronic hepatitis when hepatocyte proliferation is inhibited (17). An increase in OV-6<sup>+</sup> oval cells was indeed identified in >8- to 10-mo-old  $\beta$ -catenin KO mouse livers compared with 2- to 4-mo-old livers (SI Appendix, Fig. S5A and B), supporting the proliferation of oval cells in the inflammatory niche. The OV-6<sup>+</sup> oval cells were consistently detected in close proximity of the expanding  $\beta$ -catenin (+) HPCs and CK19<sup>+</sup> cholangiocytes in the portal area, in the liver of 8–10 mo  $\beta$ -catenin KO mice (Fig. 2B and C). Some OV-6<sup>+</sup> oval cells were even positive for  $\beta$ -catenin staining, which are oval cells possibly in transition to  $\beta$ -catenin (+) HPCs (Fig. 2D). These results thus suggest the oval cells as potential origin cells for the

expanding periportal HPCs and ductular cholangiocytes in this animal model.

Immunostaining showed an enrichment of CD45<sup>+</sup> inflammatory cells consistently associated in close proximity to the clusters of senescent hepatocytes and  $\beta$ -catenin (+) HPCs (SI Appendix, Fig. S6A). Interestingly, different classes of inflammatory cells were identified adjacent to the senescent hepatocytes or proliferating HPCs. CD11b<sup>+</sup> monocytes and CD3<sup>+</sup> T cells were found close to the senescent hepatocytes but rarely around the HPCs; the F4/80<sup>+</sup> macrophages, although distributed throughout the liver lobules, were frequently identified in close contact with the HPCs (SI Appendix, Fig. S6B and C).

Overall, this  $\beta$ -catenin KO mouse model closely duplicates the expansion of periportal HPCs in the senescence-associated human livers with chronic hepatitis.

**Complement C1q Is Elevated in the Inflammatory Niche as a Candidate Factor that Activates the  $\beta$ -Catenin Pathway in Periportal HPCs.**

With the aim of identifying the genes/pathways that promote the proliferation of HPCs in this inflammatory liver, we compared the gene expression profiles in livers from control wild-type (WT) mice and  $\beta$ -catenin KO mice at different ages using a microarray analysis. The candidate factors previously reported to be involved in regulating HPC proliferation, including IL-6, TWEAK, TGF- $\beta$ , HGF, FGF7, and Wnt ligands (9, 18, 19), did not show significant changes. Instead, a prominent elevation in the expression levels of complement component C1q (including subunits C1qa, C1qb, and C1qc) was commonly identified in the livers of 10- and 18-mo-old  $\beta$ -catenin KO mice by Biocarta, GeneMAPP, and KEGG analyses (SI Appendix, Table S1 and Fig. 3A). The elevated C1q expression in the liver tissues of >9- to 10-mo-old  $\beta$ -catenin KO mice was verified by qRT-PCR, Western blot analysis, and IHC staining (Fig. 3B–D). As documented, C1q consists of subunits C1qa, C1qb, and C1qc and is produced by macrophages and dendritic cells (20). Immunostaining of the liver tissues in >9- to 10-mo-old  $\beta$ -catenin KO mice revealed C1q expression in some inflammatory cells, mainly the F4/80<sup>+</sup> macrophages rather than the CD11b<sup>+</sup> monocytes around the proliferating  $\beta$ -catenin (+) HPCs (Fig. 3E–G).

In addition to C1q's function as the initiator for the classical complement system (21), a recent study identified a novel function of C1q in the activation of the canonical Wnt pathway by binding to Frizzled receptors to activate C1r and C1s, which cleaves the ectodomain of LRP6 to trigger the  $\beta$ -catenin pathway (22). A positive signal for GS, a target gene for the  $\beta$ -catenin pathway in liver, supports activation of the  $\beta$ -catenin pathway, a major factor responsible for the proliferation and stemness of progenitor cells (23), in the expanding periportal HPCs (Fig. 3H and SI Appendix, Fig. S7A). However, expression levels of the classical Wnt ligands, including Wnt3, Wnt3a, Wnt2, Wnt9b, Wnt1, Wnt5a, Wnt11, Wnt7a, Wnt7b, and Wnt10a, that could activate the  $\beta$ -catenin pathway in HPCs, were not elevated in the livers of 10- and 18-mo-old  $\beta$ -catenin KO mice (SI Appendix, Fig. S7B). Instead, C1q and C1q-producing F4/80<sup>+</sup> macrophages were enriched in the inflammatory microenvironment, including those surrounding the GS<sup>+</sup> HPCs (Fig. 3I and SI Appendix, Fig. S6C). Thus, we performed IF staining with the phospho-LRP6 (S1490) Ab, which recognizes phosphorylated Ser in PPPSP motifs (24), in liver tissues of 10-mo-old WT and  $\beta$ -catenin KO mice. As an indicator of activation of the LRP6 mediated  $\beta$ -catenin pathway (25), the WT control mice showed a positive phospho-LRP6 (pLRP6) signal in hepatocytes only in the peri-central area. In contrast, the cluster of  $\beta$ -catenin (+) HPCs at the portal area in  $\beta$ -catenin KO mice showed a pLRP6 signal in association with the C1q signals. These findings support LRP6-mediated activation of the  $\beta$ -catenin pathway coupled with C1q expression in the portal HPCs at the inflammatory microenvironment in  $\beta$ -catenin KO mice (SI Appendix, Fig. S8). Therefore, we proposed that C1q might function as a candidate unorthodox

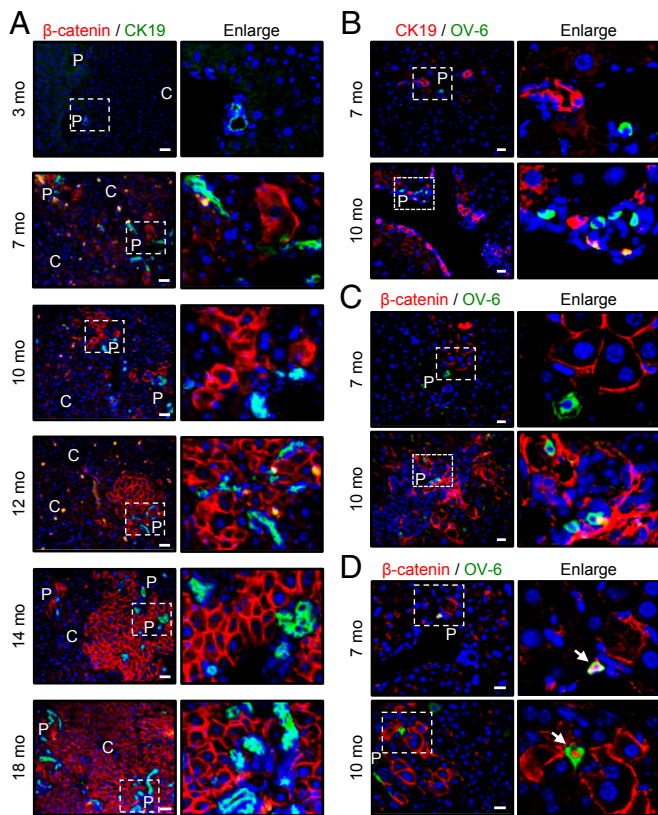


**Fig. 2.** Expansion of HPCs is from the periportal area to the central region and is associated with bile duct reactions in  $\beta$ -catenin KO mice. The liver tissues obtained from  $\beta$ -catenin KO mice at different ages were processed for IF staining with  $\beta$ -catenin and CK19 (A), CK19 and OV-6 (B), and  $\beta$ -catenin and OV-6 (C and D) antibodies. P, portal area; C, central vein area. White arrows in (D) indicate the cells coexpressing  $\beta$ -catenin and OV-6 proteins. (Scale bars: 50  $\mu$ m for A; 20  $\mu$ m for B–D.)

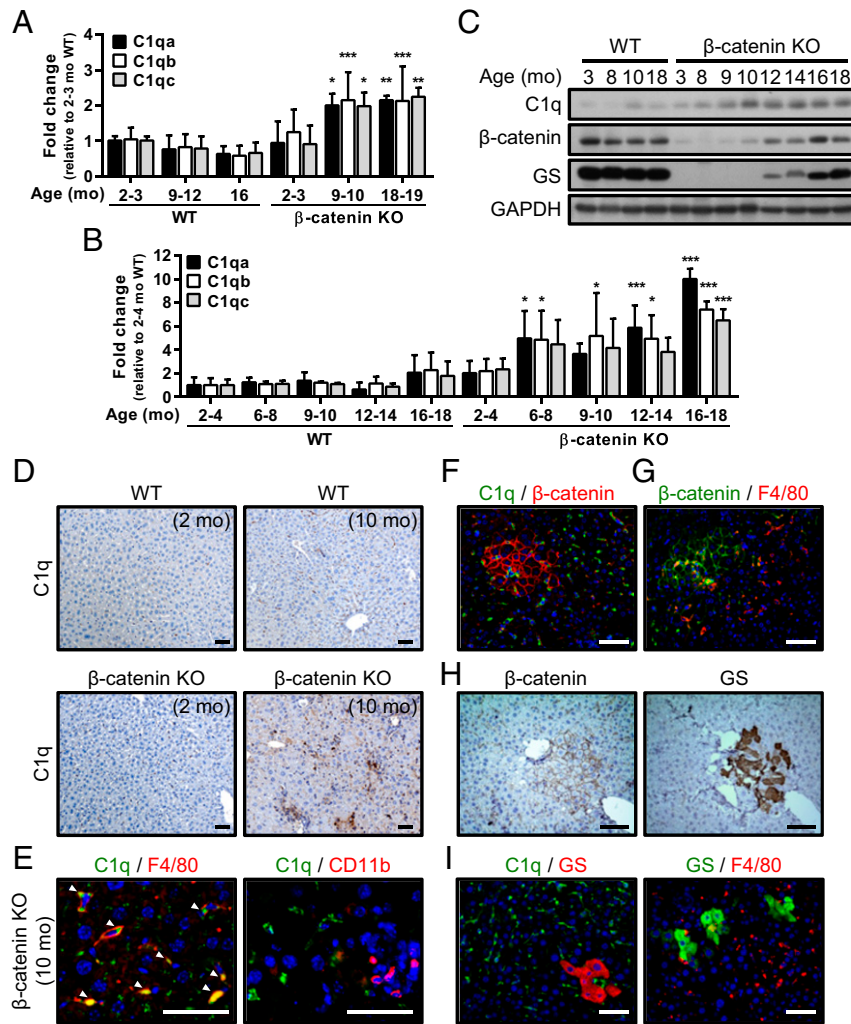


**Fig. 3.** Complement C1q levels are elevated in the inflammatory niche and associated with activation of the  $\beta$ -catenin pathway in periportal HPCs. (A) Results of the microarray analysis showing the levels of the C1qa, C1qb, and C1qc mRNAs in liver tissues collected from WT control and  $\beta$ -catenin KO mice at the indicated ages. The levels were compared with the 2- to 3-mo-old WT livers, in which the level was set to 1.  $n = 3$  to 6 per group. (B and C) qRT-PCR data (B) and representative Western blots (C) showing C1q expression in the liver tissues of WT and  $\beta$ -catenin KO mice at various ages. Levels of C1qa, C1qb, and C1qc mRNA were compared between the  $\beta$ -catenin KO livers and WT livers at 2 to 4 mo. Results are presented as mean  $\pm$  SD. \* $P < 0.05$ ; \*\* $P < 0.01$ ; \*\*\* $P < 0.001$ .  $n = 3$  to 5 per group. (D) IHC staining with C1q antibody in the liver tissues collected from 2- and 10-mo-old WT and  $\beta$ -catenin KO mice. (E) IF staining for C1q, F4/80, and CD11b in liver tissues of 10-mo-old  $\beta$ -catenin KO mice. White arrowheads indicate the colocalization of C1q and F4/80. (F–I) Representative IF and IHC staining with indicated antibodies in 10- to 12-mo-old  $\beta$ -catenin KO liver tissues. (Scale bars: 50  $\mu$ m.)

factor from the inflammatory niche that activates the  $\beta$ -catenin pathway in HPCs, thus maintaining their proliferation in the  $\beta$ -catenin KO mouse livers.

**Inhibition of C1q Suppressed the Expansion but Facilitated the Differentiation of HPCs by Inhibiting Activity of the  $\beta$ -Catenin Pathway.** To test our hypothesis, we attempted to block C1q activity using two C1q inhibitors, the 2J synthetic peptide (26) and low molecular weight dextran sulfate (DXS) (27). We first i.p. injected the 2J peptide into the 7-mo-old  $\beta$ -catenin KO mice, the age around which the inflammatory niche forms. The efficacy of this treatment was confirmed by a decrease in serum complement C3a levels (Fig. 4A). Interestingly, liver weight was decreased by  $\sim 20\%$  over the 2-mo treatment compared with the untreated mice (Fig. 4B). The numbers of both the  $\beta$ -catenin (+) and GS<sup>+</sup> HPCs were also significantly decreased in the livers of 2J peptide-treated  $\beta$ -catenin KO mice, as indicated by IF staining (Fig. 4C) and Western blot analysis (Fig. 4D). A similar effect was observed on HPCs from  $\beta$ -catenin KO

mice treated with another C1q inhibitor, DXS (SI Appendix, Fig. S9A–C). Thus, treatments with C1q inhibitors might reduce the proliferation of HPCs by inhibiting the activity of the  $\beta$ -catenin pathway.

We then examined whether the  $\beta$ -catenin (+) HPCs undergo terminal differentiation in response to the C1q inhibitor treatment, which might elevate albumin-Cre expression to a level sufficient for depleting  $\beta$ -catenin expression. The genomic DNA analysis showed a significantly higher lox-P-mediated recombination efficiency in both the 2J peptide- and DXS-treated  $\beta$ -catenin KO livers compared with the untreated KO mouse livers (Fig. 4E for the 2J peptide; SI Appendix, Fig. S9D for DXS). The results indicate a role for C1q in maintaining the dedifferentiated state of the expanded HPCs in  $\beta$ -catenin KO mice.

As a control experiment, the effect of DXS and 2J peptide on the  $\beta$ -catenin pathway activity in the pericentral hepatocytes was examined in the WT control mice by analyzing the expression of GS protein. Neither the IHC or the Western blot analysis showed any effect on GS from treatment with DXS and 2J peptide (Fig. 4

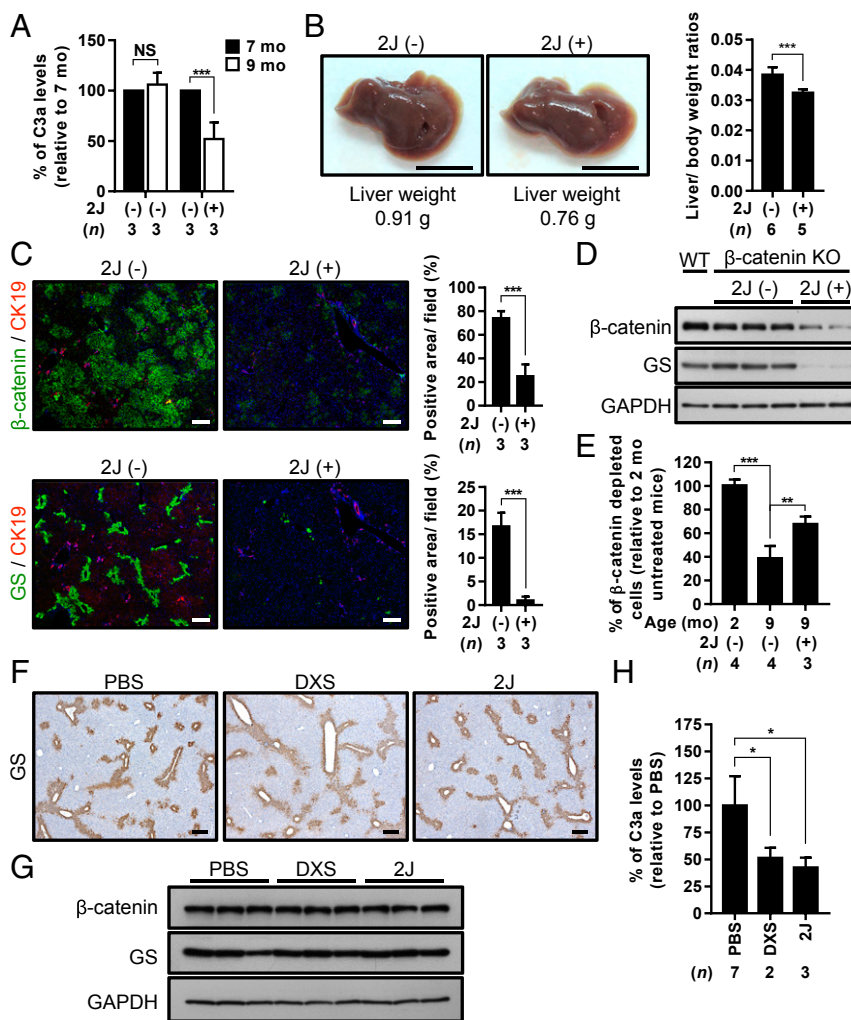


**Fig. 4.** Inhibition of C1q suppresses the expansion of periportal HPCs in  $\beta$ -catenin KO mice. (A) C3a levels in serum samples collected from  $\beta$ -catenin KO mice before (7 mo) and after (9 mo) 2J peptide treatment, as determined by enzyme-linked immunosorbent assay. (B) Representative images of the gross view, liver weights (Left) and liver-to-body weight ratios (Right) of 9-mo-old  $\beta$ -catenin KO mice with and without 2J peptide treatment. (C) Representative images of IF staining for the indicated antibodies in continuous liver tissue sections collected from 9-mo-old  $\beta$ -catenin KO mice with and without 2J peptide treatment. Percentages of  $\beta$ -catenin (+) and GS(+) areas were quantified and are shown in bar graphs to the right of the staining results. (D) Western blots showing the expression of  $\beta$ -catenin and GS in liver tissues collected from 9-mo-old  $\beta$ -catenin KO mice with and without 2J peptide treatment.  $\beta$ -catenin and GS expression in the liver tissues from age-matched WT control mice served as a positive control. (E) Genomic DNA was extracted from liver tissues collected from untreated and 2J peptide-treated  $\beta$ -catenin KO mice and processed for qRT-PCR analysis using primer sets that differentiated the occurrence of Cre-loxP recombination to examine the percentage of cells in which  $\beta$ -catenin was deleted in each liver tissue. The percentage observed in the livers of 2-mo-old  $\beta$ -catenin KO mice was set to 100%. (F) Representative IHC staining for GS in the liver tissues collected from 9-mo-old WT mice treated with PBS, DXS, or 2J peptide. (G) Western blot showing the expression of  $\beta$ -catenin and GS in the liver tissues of WT mice treated with indicated inhibitors. (H) C3a levels in serum samples collected from WT mice after treatment with PBS, DXS, and 2J peptide. Results are presented as mean  $\pm$  SD. N.S., not significant. \* $P < 0.05$ ; \*\* $P < 0.01$ ; \*\*\* $P < 0.001$ . (Scale bars: 1 cm for B; 200  $\mu$ m for C and F.)

F and G), although the efficacy was validated by a decrease in C3a (Fig. 4H). This indicates that targeting the unorthodox signal C1q in the inflammatory niche selectively blocked the  $\beta$ -catenin mediated expansion of HPCs but spared its physiological functions regulated by the orthodox Wnt signals in pericentral hepatocytes.

**Liver Tumors Containing WT  $\beta$ -Catenin Are Responsive to C1q Inhibitor Treatment.** As shown in our previous study, HBx accelerates the replacement event for HPCs and the subsequent carcinogenesis (12). In the HBx transgenic (HBx-Tg)/ $\beta$ -catenin KO mice, we found that the proliferation of HPCs was also predisposed by the senescence of hepatocytes, with increases in hepatocytes positive for SA- $\beta$ -gal, p21, and p16 (SI Appendix, Fig. S10A). Elevated C1q expression was also associated with the replacement event in this animal model at an earlier age ( $\sim$ 2 mo) (SI Appendix, Fig. S10 B and C). The effect of the C1q inhibitors on suppression of HPC

proliferation was also consistently identified in the 3- and 6-mo-old HBx-Tg/ $\beta$ -catenin KO mice (SI Appendix, Fig. S10 D and E).

We attempted to examine the effects of the C1q inhibitors on liver tumors in  $\beta$ -catenin KO and HBx-Tg/ $\beta$ -catenin KO mice, which contain either WT or the mutant  $\beta$ -catenin (clustering at exon 3 as in human HCC) (28). Interestingly, a significant decrease in the Ki67 signal was observed in WT  $\beta$ -catenin-containing tumors but not in mutant  $\beta$ -catenin-containing tumors after treatment with the 2J peptide (Fig. 5A), suggesting decreased proliferation of the WT  $\beta$ -catenin-containing tumor cells. Meanwhile, the inhibitor treatment significantly decreased the percentage of  $\beta$ -catenin (+) cells in the WT  $\beta$ -catenin-containing tumors but not in the mutant  $\beta$ -catenin-containing tumors, as supported by the IHC staining and Western blot analysis results (Fig. 5 B and C). Thus, the WT  $\beta$ -catenin-containing tumor cells might proceed toward terminal differentiation. Indeed, the albumin-Cre-driven



recombination in the WT  $\beta$ -catenin-containing tumors was significantly increased by the treatment (Fig. 5D). These results demonstrate that the WT  $\beta$ -catenin-containing liver tumors that developed in  $\beta$ -catenin KO or HBx-Tg/ $\beta$ -catenin KO mice also responded to the C1q inhibitor treatment.

**Increased C1q Expression in the Liver Tissues of Patients with Virus-Induced Senescence-Associated Hepatitis.** Finally, we examined this novel mechanism identified in the  $\beta$ -catenin KO mice in human specimens. We analyzed the expression of C1q in 146 pairs of HCC tissues with differing viral etiologies, including HBV- and HCV-related hepatitis, as well as in 9 hemangioma and 14 focal nodular hyperplasia (FNH) specimens (which served as a normal control). As revealed by qRT-PCR, C1q expression was elevated in the nontumor portion of livers from patients with HBV- and HCV-related HCC compared with the control normal livers from patients with hemangioma and FNH (Fig. 6A). This elevated C1q expression in the nontumorous liver tissues of hepatitis patients has been supported by data from the Gene Expression Omnibus (GEO) database, including accession nos. GSE83148 (for HBV hepatitis patients) and GSE14323 (for HCV hepatitis patients) (SI Appendix, Fig. S11 A and B;  $P < 0.001$ ).

This elevated C1q expression was further validated by IHC staining. Abundant C1q<sup>+</sup> inflammatory cells, most likely macrophages, were identified in the nontumor portion of the livers from patients with HBV- and HCV-related HCC, but few such cells were found in the normal liver tissues from patients with hemangioma (Fig. 6B). Most of the C1q-enriched hepatitis liver also showed severe bile duct reactions at the periportal area, suggesting the proliferation of HPCs (Fig. 6C).

We also examined the RNA levels of p21, a marker of cellular senescence, in the nontumorous liver tissues of patients with HBV- and HCV-related HCC by qRT-PCR. The results showed a significant association between the RNA levels of C1q and p21 in both HBV- and HCV-infected patients (Fig. 6D), indicating that C1q elevation is associated with senescence of hepatic livers. This association has also been validated by data from the GEO database, including accession nos. GSE83148 (for HBV hepatitis patients) and GSE14323 (for HCV hepatitis patients) (SI Appendix, Fig. S11C;  $P < 0.001$ ).

Finally, we examined the expression pattern of GS in liver tumors from these HCC patients by IHC staining, and found elevated GS expression in ~70% of these tumors. Approximately 40% of the GS<sup>+</sup> HCCs developed in the C1q and bile duct reaction-enriched liver contained the WT  $\beta$ -catenin (Fig. 6E).

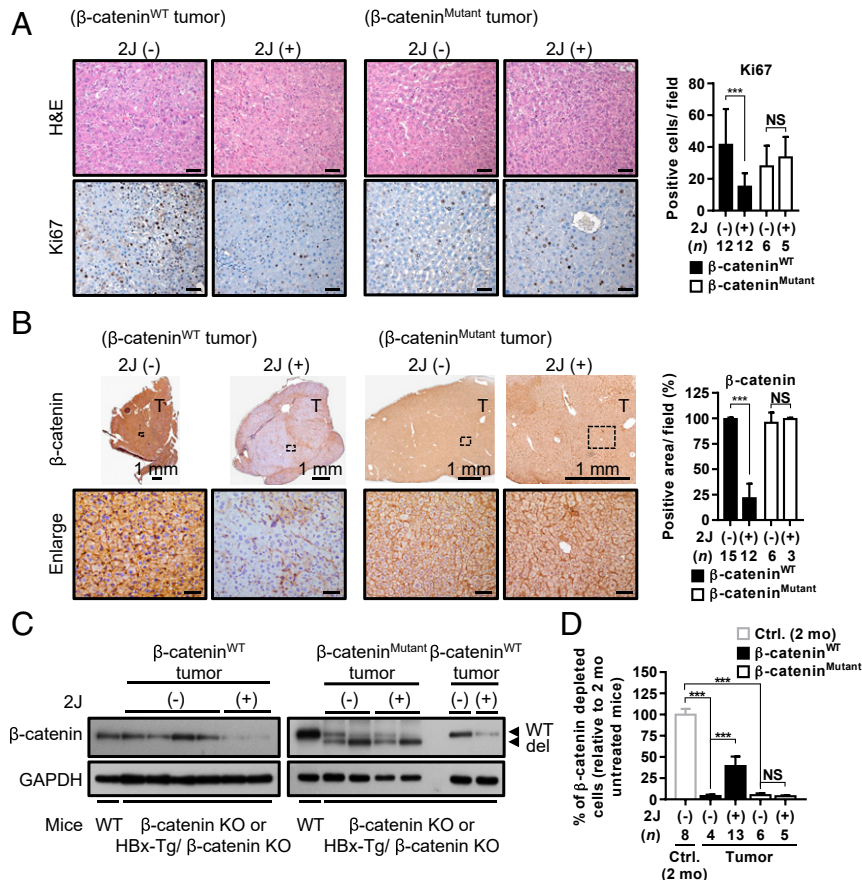


**Fig. 5.** Liver tumors containing WT  $\beta$ -catenin are responsive to C1q inhibitor treatment. (A and B) Representative images of H&E and IHC staining for Ki67 (A) and  $\beta$ -catenin (B) in WT and mutant  $\beta$ -catenin-containing liver tumors from  $\beta$ -catenin KO and HBx-Tg/ $\beta$ -catenin KO mice that were not treated or treated with 2J peptide for 2 mo. Percentages of positive signals for Ki67 and  $\beta$ -catenin were quantified and are shown as bar graphs to the right of the images. (C) Western blots showing the expression of  $\beta$ -catenin in WT and mutant  $\beta$ -catenin-containing liver tumors collected from untreated or 2J peptide-treated tumor-bearing mice.  $\beta$ -catenin expression in the liver tissues of WT control mice served as a positive control. (D) Genomic DNA extracted from the liver tissues collected from different groups of mice as indicated were processed for qRT-PCR analysis to evaluate the percentage of cells in which  $\beta$ -catenin was depleted in each liver tissue. The percentage of  $\beta$ -catenin depletion in the liver tissues from 2-mo-old  $\beta$ -catenin KO mice was set to 100%. The  $\beta$ -catenin mutations identified in the tumors were mutations or deletions at around exon 3 of the *CTNNB1* gene. Results are presented as mean  $\pm$  SD. N.S., not significant. \*\*\* $P < 0.001$ . (Scale bar: 50  $\mu$ m for A and B.)

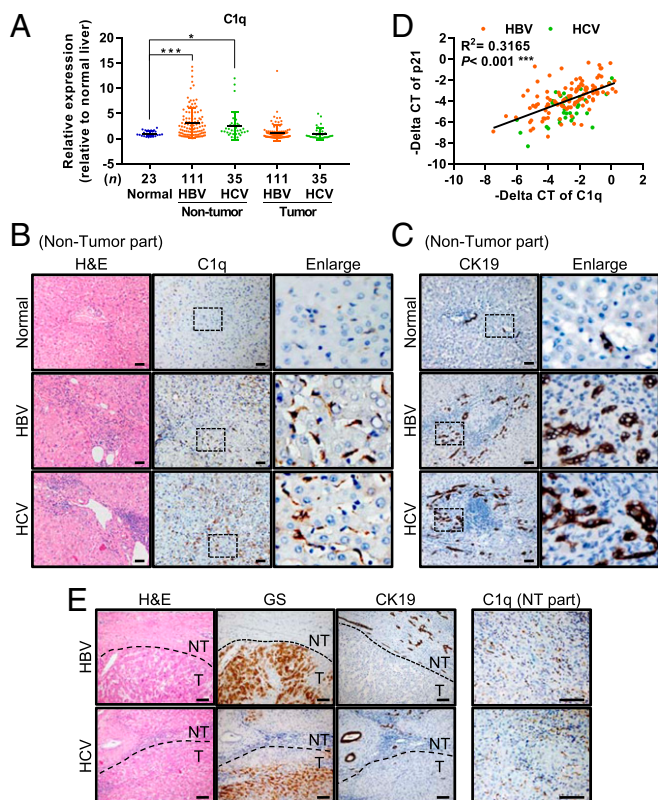


**Fig. 6.** Abundant C1q-expressing inflammatory cells are present in the nontumor regions of liver tissues from patients with viral infection-related HCC. (A) qRT-PCR of C1q in the nontumor and tumor liver tissues collected from patients with HBV- and HCV-related HCC. The nontumor liver tissues collected from patients with hemangioma or FNH were included as normal liver controls. Results are presented as mean  $\pm$  SD. \* $P < 0.05$ ; \*\*\* $P < 0.001$ . (B and C) Representative images of H&E and IHC staining for C1q (B) and CK19 (C) in the normal liver tissues and nontumorous liver tissues from patients with HBV- and HCV-related HCC. (D) Association between the mRNA levels of C1q and p21 in the nontumor liver tissues of patients with HBV- and HCV-related HCC. (E) Representative images of the H&E and IHC staining for GS, CK19, and C1q in the paired nontumorous (NT) and tumorous (T) liver tissues collected from patients with HBV- and HCV-related HCC. (Scale bars: 50  $\mu$ m for B and C; 100  $\mu$ m for E.)

Taken together, these results support the idea that the mechanism identified in the  $\beta$ -catenin KO mouse model might be present in the human specimens as well.

## Discussion

Chronic hepatitis causes the death of hepatocytes, followed by active growth of residual cells in the inflammatory niche and subsequent development of liver tumors. When hepatocyte proliferation is blocked, as in the case of severe senescence-associated hepatitis induced by hepatitis virus infection, small cells with scant cytoplasm and oval-shaped nuclei (oval cells) located in the canal of Hering proliferate at the periportal area. This has long been considered the major source of compensatory regeneration and subsequent liver tumors (29). Despite extensive studies, the signal from the inflammatory niche required for expansion of these HPCs has remained poorly characterized. Our study demonstrates that the hepatic  $\beta$ -catenin KO mice is a useful model for studying the underlying mechanism. Depletion of the essential  $\beta$ -catenin leads the hepatocytes to senescence at the end of their life span, which induces an inflammatory microenvironment for HPC regeneration from the periportal oval cells. A recent study consistently showed a compensatory regeneration of

hepatocytes from biliary cells when the hepatocyte proliferation is impaired by p21 overexpression (30).

Based on the evidence obtained from different animal models, various signals from the inflammatory niche have been shown to be involved in the proliferation of progenitor cells in the liver, including IL-6, TWEAK, and Wnt3a released from macrophages and TGF- $\beta$ , HGF, and FGF7 released from hepatic stellate cells (31). Previous studies have suggested that HGF and IL-6 could regulate the proliferation of progenitor cells through the PI3K/AKT and STAT3 signaling pathway (32, 33) and that Wnt3a and TGF- $\beta$  signaling might activate the  $\beta$ -catenin pathway in HPCs (31, 34). In addition, a group of diploid hepatocytes adjacent to the central veins were recently shown to have self-renewing activity, which is triggered by the Wnt ligands secreted from the endothelial cells lining the central veins (3). Interestingly, our microarray data do not show significant changes in the expression levels of these putative factors or the conventional Wnt ligands in the livers of aging  $\beta$ -catenin KO mice, but instead reveal elevated expression levels of complement C1q.

The complement system is an enzymatic cascade initiated by the interaction of C1q with immune complexes to form a lytic complex at the cell membrane, which kills and clears the targeted cells (21). The effect is generally considered a host defense mechanism for eliminating pathogen-infected cells. Interestingly, the concentration of C1q in serum and its expression levels in various tissues were found to be elevated during the aging process, possibly as a mechanism to activate the  $\beta$ -catenin pathway in aging cells (22). Our present study shows that this mechanism works to regulate the expansion and dedifferentiation of HPCs in the senescence-associated inflammatory liver. As C1q staining was very low in nontumor tissues from patients with hepatic hemangioma and FNH but quite prominent in these tissues from patients with chronic hepatitis B and C patients, the macrophages producing high levels of C1q are not likely to be residential Kupffer cells, and may be influx circulatory monocytes/macrophages attracted by the SASP factors released by the senescent cells.

We further validated this mechanism in human specimens. The number of C1q-secreting macrophages was significantly increased in the nontumor region of liver tissues from patients with HBV- and HCV-induced HCC, in which many hepatocytes undergo senescence and trigger an associated inflammatory microenvironment. The viral etiology for promoting the proliferation of periportal HPCs might be triggered by the senescence of hepatocytes induced by viral infection, with previous microarray analyses also showing higher C1q expression levels in the livers of patients with chronic hepatitis B, rapidly normalize serum aminotransferase levels by reducing virus-induced inflammation and the associated HCC risk. Their efficacy may be related to the suppression of C1q-mediated HPC proliferation suggested in our study, which warrants further investigation.

Blockade of this unorthodox signal with C1q inhibitors significantly decreased the proliferation of HPCs. Moreover, the HPCs that already existed in the inflammatory environment might have undergone terminal differentiation after discontinuation of the  $\beta$ -catenin signaling pathway. Therefore, C1q-activated  $\beta$ -catenin contributes to increased proliferation and dedifferentiation of HPCs in the liver of patients with hepatitis. This mechanism is apparently distinct from the effects of the orthodox Wnt signals on the pericentral hepatocytes in the normal liver, which undergo terminal differentiation soon after proliferation (3). Subsequent studies of tumor development in this  $\beta$ -catenin KO mouse model after long-term C1q inhibitor treatment will be interesting.

Of note, our study further indicates that not only the HPCs, but also the liver tumors containing WT but not mutant  $\beta$ -catenin

in either  $\beta$ -catenin KO or HBx-tg/ $\beta$ -catenin KO mice were responsive to the C1q inhibitor treatment. The number of  $\beta$ -catenin (+) tumor cells in the liver tumors was significantly decreased, from  $\sim$ 100% to  $\sim$ 30%, after 30 d of treatment. This decrease in the number of  $\beta$ -catenin (+) tumor cells and associated increase in Cre-mediated recombination events support the hypothesis that the WT  $\beta$ -catenin-containing tumor cells might undergo terminal differentiation in response to the inhibitor treatment, similar to that of HPCs. As documented, the  $\beta$ -catenin pathway is active in  $>$ 70% of HBV-related HCCs, but in only  $\sim$ 20% of those containing the mutant  $\beta$ -catenin (28). Although HCCs containing mutant  $\beta$ -catenin are more frequent in HCV-related HCC, mutation-independent activation of  $\beta$ -catenin remains in a significant proportion of HCCs, especially in HBV-related HCCs (37). Our study suggests that most of the WT  $\beta$ -catenin-containing liver tumors in the  $\beta$ -catenin KO and HBx-tg/ $\beta$ -catenin KO mice might develop in a C1q-dependent manner. Therefore, C1q could be a candidate for activating the WT  $\beta$ -catenin in HCC and may become a potential therapeutic target for such HCCs. Further follow-up of the tumors developed in this  $\beta$ -catenin KO mouse model after long-term C1q inhibitor treatment may help clarify whether the progression of WT  $\beta$ -catenin-containing liver tumors can be diminished by C1q inhibitor treatment.

In addition to the development of tankyrase inhibitors, such as XAV939 and IWR-1, with the ability to accelerate the degradation of  $\beta$ -catenin, several small molecules have been developed to inhibit the  $\beta$ -catenin pathway by targeting multiple components in this pathway (38). For example, LGK974 inhibits the secretion of Wnt ligands by blocking the porcupine acyltransferase (39), and ICG-001 and PRI-724 block the interaction of  $\beta$ -catenin with the transcriptional coregulators CBP and TCF (40). However, none of these compounds specifically inhibits the aberrant oncogenic activation of the Wnt pathway. Therefore, they might also affect its physiological function in normal cells and cause systemic side effects. In contrast, treatment with C1q inhibitors suppresses only the Wnt pathway in HPCs in the inflammatory niche but spares the normal ones in zone 3 functions, as shown in the WT control mice. Our results thus highlight the advantage of this class of Wnt inhibitors that target C1q to suppress the  $\beta$ -catenin pathway in periportal HPCs specifically located in the inflammatory niche, which inhibits their continuous proliferation and long-lasting stemness. Therefore, this C1q mechanism provides a therapeutic target for future drug development to specifically block inflammation-induced HPC proliferation and subsequent development of HCC. In the present study, two complement inhibitors, DXS and peptide 2J, worked well in our animal model to block  $\beta$ -catenin activity in HPCs and could be candidates for further drug development. In addition, there are several

complement component inhibitors under development (41) that can be tested in the future.

## Materials and Methods

Detailed descriptions of the materials and methods used in this study, including antibodies used, protein and RNA analyses, immunostaining, senescence-associated SA- $\beta$ -gal assay, microarray analysis, isolation of non-parenchymal cells, flow cytometry analysis, complement C3a analysis, GEO dataset analysis, and statistical analysis, are provided in *SI Appendix*.

**Hepatocyte-Specific  $\beta$ -Catenin KO Mice and HBx Transgenic (Tg) Mice.** All animal studies were conducted in accordance with the guidelines of the Association for Assessment and Accreditation of Laboratory Animal Care and approved by the Institutional Animal Care and Use Committee at the National Taiwan University College of Medicine. All the mice were bred and analyzed in a specific pathogen-free facility. The transgenic mice with the hepatocyte-specific albumin promoter-driven Cre recombinase (*Alb-Cre* mice, C57BL/6) and the floxed  $\beta$ -catenin (exons 2 to 6) (*Ctnnb1<sup>flx/flx</sup>* mice, C57BL/6) were obtained from The Jackson Laboratory (stock nos. 003574 and 004152). The HBx-Tg mice were generated by pronucleus microinjection of C57BL/6 fertilized eggs with a HBx gene expression construct (in pAlb-In-pA-HS4 vector), with its expression driven by the albumin promoter (42). The hepatocyte-specific HBx-Tg and  $\beta$ -catenin KO mice were generated by crossing the hepatocyte specific  $\beta$ -catenin KO mice with HBx-Tg mice. Breeding and genotyping were done as described previously (12).

**Inhibitor Treatment.** Low molecular weight DXS (D7037; Sigma-Aldrich) and 2J peptide (synthesized by Mission Biotech) were delivered into the mice by i.v. tail vein injection or i.p. injection twice weekly at concentrations of 30 mg/kg and 2 mg/kg, respectively.

**Clinical Specimens.** Paired liver tissues from 9 hemangioma, 14 FNH, 111 HBV-related HCC, and 35 HCV-related HCC patients collected in the Taiwan Liver Cancer Network were included in this study. RNA extracted from the frozen tissues was processed for qRT-PCR analysis, and liver tissue sections were processed for the H&E and IHC staining. The Institutional Review Board of National Taiwan University Hospital approved the use of these archived tissues.

**Data Availability.** All data discussed in the paper are included in the manuscript and *SI Appendix*.

**ACKNOWLEDGMENTS.** We thank the Taiwan Liver Cancer Network for providing samples and related data (all anonymous) for our research. We also thank the staff of the imaging core at the First Core Labs, National Taiwan University College of Medicine for technical assistance, and the Laboratory Animal Center, National Taiwan University College of Medicine for technical support in pathological analysis. We would like to acknowledge the service provided by the Flow Cytometric Analyzing and Sorting Core of the First Core Laboratory, National Taiwan University College of Medicine. This study was financially supported by grants from the Ministry of Science and Technology, Taiwan (MOST104-2314-B-002-023-MY3, MOST107-2321-B-001-025, MOST108-3017-F-002-004, and MOST108-2314-B-002-141-MY3), the National Taiwan University (NTU103C101-12) and the Center of Precision Medicine from The Featured Areas Research Center Program within the framework of the Higher Education Sprout Project of the Ministry of Education in Taiwan.

1. A. I. Gomaa, S. A. Khan, M. B. Toledano, I. Waked, S. D. Taylor-Robinson, Hepatocellular carcinoma: Epidemiology, risk factors and pathogenesis. *World J. Gastroenterol.* **14**, 4300–4308 (2008).
2. G. C. Leonardi *et al.*, The tumor microenvironment in hepatocellular carcinoma (review). *Int. J. Oncol.* **40**, 1733–1747 (2012).
3. B. Wang, L. Zhao, M. Fish, C. Y. Logan, R. Nusse, Self-renewing diploid Axin2(+) cells fuel homeostatic renewal of the liver. *Nature* **524**, 180–185 (2015).
4. E. S. Park *et al.*, Hepatitis B virus inhibits liver regeneration via epigenetic regulation of urokinase-type plasminogen activator. *Hepatology* **58**, 762–776 (2013).
5. A. Marshall *et al.*, Relation between hepatocyte G1 arrest, impaired hepatic regeneration, and fibrosis in chronic hepatitis C virus infection. *Gastroenterology* **128**, 33–42 (2005).
6. T. Roskams, Liver stem cells and their implication in hepatocellular and cholangiocarcinoma. *Oncogene* **25**, 3818–3822 (2006).
7. J. Font-Burgada *et al.*, Hybrid periportal hepatocytes regenerate the injured liver without giving rise to cancer. *Cell* **162**, 766–779 (2015).
8. C. Wang *et al.*, Hepatitis B virus X (HBx) induces tumorigenicity of hepatic progenitor cells in 3,5-diethoxycarbonyl-1,4-dihydrocollidine-treated HBx transgenic mice. *Hepatology* **55**, 108–120 (2012).
9. W. Y. Lu *et al.*, Hepatic progenitor cells of biliary origin with liver repopulation capacity. *Nat. Cell Biol.* **17**, 971–983 (2015).
10. S. U. Wiemann *et al.*, Hepatocyte telomere shortening and senescence are general markers of human liver cirrhosis. *FASEB J.* **16**, 935–942 (2002).
11. A. D. Aravinthan, G. J. M. Alexander, Senescence in chronic liver disease: Is the future in aging? *J. Hepatol.* **65**, 825–834 (2016).
12. E. Y. Wang *et al.*, Depletion of  $\beta$ -catenin from mature hepatocytes of mice promotes expansion of hepatic progenitor cells and tumor development. *Proc. Natl. Acad. Sci. U.S.A.* **108**, 18384–18389 (2011).
13. J. O. Russell *et al.*, Hepatocyte-specific  $\beta$ -catenin deletion during severe liver injury provokes cholangiocytes to differentiate into hepatocytes. *Hepatology* **69**, 742–759 (2019).
14. T. Eggert *et al.*, Distinct functions of senescence-associated immune responses in liver tumor surveillance and tumor progression. *Cancer Cell* **30**, 533–547 (2016).
15. T. W. Kang *et al.*, Senescence surveillance of pre-malignant hepatocytes limits liver cancer development. *Nature* **479**, 547–551 (2011).
16. J. Yang, L. Zhang, C. Yu, X. F. Yang, H. Wang, Monocyte and macrophage differentiation: Circulation inflammatory monocyte as biomarker for inflammatory diseases. *Biomark. Res.* **2**, 1 (2014).
17. M. Okabe *et al.*, Potential hepatic stem cells reside in EpCAM<sup>+</sup> cells of normal and injured mouse liver. *Development* **136**, 1951–1960 (2009).
18. M. Kitade, K. Kajii, H. Yoshiji, Relationship between hepatic progenitor cell-mediated liver regeneration and non-parenchymal cells. *Hepatol. Res.* **46**, 1187–1193 (2016).



19. G. He *et al.*, Identification of liver cancer progenitors whose malignant progression depends on autocrine IL-6 signaling. *Cell* **155**, 384–396 (2013).
20. G. Castellano *et al.*, Maturation of dendritic cells abrogates C1q production in vivo and in vitro. *Blood* **103**, 3813–3820 (2004).
21. A. P. Sjöberg, L. A. Trouw, A. M. Blom, Complement activation and inhibition: A delicate balance. *Trends Immunol.* **30**, 83–90 (2009).
22. A. T. Naito *et al.*, Complement C1q activates canonical Wnt signaling and promotes aging-related phenotypes. *Cell* **149**, 1298–1313 (2012).
23. K. N. Nejak-Bowen, S. P. Monga, Beta-catenin signaling, liver regeneration and hepatocellular cancer: Sorting the good from the bad. *Semin. Cancer Biol.* **21**, 44–58 (2011).
24. K. Tamai *et al.*, A mechanism for Wnt coreceptor activation. *Mol. Cell* **13**, 149–156 (2004).
25. B. T. MacDonald, X. He, Frizzled and LRP5/6 receptors for Wnt/ $\beta$ -catenin signaling. *Cold Spring Harb. Perspect. Biol.* **4**, a007880 (2012).
26. A. Roos *et al.*, Specific inhibition of the classical complement pathway by C1q-binding peptides. *J. Immunol.* **167**, 7052–7059 (2001).
27. R. Spirig, T. Gajanayake, O. Korsgren, B. Nilsson, R. Rieben, Low molecular weight dextran sulfate as complement inhibitor and cytoprotectant in solid organ and islet transplantation. *Mol. Immunol.* **45**, 4084–4094 (2008).
28. B. Cieply, G. Zeng, T. Proverbs-Singh, D. A. Geller, S. P. Monga, Unique phenotype of hepatocellular cancers with exon-3 mutations in beta-catenin gene. *Hepatology* **49**, 821–831 (2009).
29. S. Yang *et al.*, Oval cells compensate for damage and replicative senescence of mature hepatocytes in mice with fatty liver disease. *Hepatology* **39**, 403–411 (2004).
30. A. Raven *et al.*, Cholangiocytes act as facultative liver stem cells during impaired hepatocyte regeneration. *Nature* **547**, 350–354 (2017).
31. L. Boulter *et al.*, Macrophage-derived Wnt opposes Notch signaling to specify hepatic progenitor cell fate in chronic liver disease. *Nat. Med.* **18**, 572–579 (2012).
32. G. C. Yeoh *et al.*, Opposing roles of gp130-mediated STAT-3 and ERK-1/2 signaling in liver progenitor cell migration and proliferation. *Hepatology* **45**, 486–494 (2007).
33. T. Ishikawa *et al.*, Hepatocyte growth factor/c-met signaling is required for stem-cell-mediated liver regeneration in mice. *Hepatology* **55**, 1215–1226 (2012).
34. A. Ceulemans *et al.*, RNA-sequencing-based comparative analysis of human hepatic progenitor cells and their niche from alcoholic steatohepatitis livers. *Cell Death Dis.* **8**, e3164 (2017).
35. F. Bohne *et al.*, HCV-induced immune responses influence the development of operational tolerance after liver transplantation in humans. *Sci. Transl. Med.* **6**, 242ra81 (2014).
36. W. Zhou *et al.*, Predictive model for inflammation grades of chronic hepatitis B: Large-scale analysis of clinical parameters and gene expressions. *Liver Int.* **37**, 1632–1641 (2017).
37. M. L. Tornesello *et al.*, Mutations in TP53, CTNNB1, and PIK3CA genes in hepatocellular carcinoma associated with hepatitis B and hepatitis C virus infections. *Genomics* **102**, 74–83 (2013).
38. N. Krishnamurthy, R. Kurzrock, Targeting the Wnt/ $\beta$ -catenin pathway in cancer: Update on effectors and inhibitors. *Cancer Treat. Rev.* **62**, 50–60 (2018).
39. S. Ortica, N. Tarantino, N. Aulner, A. Israël, N. Gupta-Rossi, The 4 Notch receptors play distinct and antagonistic roles in the proliferation and hepatocytic differentiation of liver progenitors. *FASEB J.* **28**, 603–614 (2014).
40. S. Khurana, A. Mukhopadhyay, Hematopoietic progenitors from early murine fetal liver possess hepatic differentiation potential. *Am. J. Pathol.* **173**, 1818–1827 (2008).
41. L. Beinrohr, J. Dobó, P. Závodszy, P. Gál, C1, MBL-MASPs and C1-inhibitor: Novel approaches for targeting complement-mediated inflammation. *Trends Mol. Med.* **14**, 511–521 (2008).
42. B. K. Wu *et al.*, Blocking of G1/S transition and cell death in the regenerating liver of Hepatitis B virus X protein transgenic mice. *Biochem. Biophys. Res. Commun.* **340**, 916–928 (2006).